STOCHASTIC STABILITY AND PERFORMANCE ROBUSTNESS OF LINEAR MULTIVARIABLE SYSTEMS

Laura E. Ryan[*] and Robert F. Stengel[**]

Department of Mechanical and Aerospace Engineering
Princeton University
Princeton, N.J.

ABSTRACT

Stochastic robustness, a simple technique used to estimate the robustness of linear, time-invariant systems, is applied to a single-link robot arm control system. Concepts behind stochastic *stability* robustness are extended to systems with estimators and to stochastic *performance* robustness. Stochastic performance robustness measures based on classical design specifications are introduced, and the relationship between stochastic robustness measures and control system design parameters is discussed. The application of stochastic performance robustness, and the relationship between performance objectives and design parameters are demonstrated by means of the example. The results prove stochastic robustness to be a good overall robustness an' ·is method that can relate robustness characteristics to con.   stem design parameters.

INTRODUCTION

Standard linear control system design techniques rely on accurate models of the system to be controlled. Because models are never perfect, robustness analysis is necessary to determine the possibility of instability or inadequate performance in the face of uncertainty. Robustness to these uncertainties, parametric or unstructured, is normally treated deterministically and often without regard to possible physical variations in the system. Consequently, overconservative control system designs, or designs that are insufficiently robust in the face of real world uncertainties are a danger.

Stochastic robustness, a simple technique to determine the robustness of linear, time-invariant systems by Monte Carlo methods was introduced in [1] and presented in detail in [2,3]. These references described stochastic stability robustness analysis and introduced the probability of instability as a scalar measure of stability robustness. Confidence intervals for the scalar probability of instability were presented, and the stochastic root locus, or probability density of the closed-loop eigenvalues, has shown to portray robustness properties graphically. Because it is a statistical measure of robustness, and because it directly uses knowledge of the statistics of the physical parameter variations, stochastic robustness is inherently intuitive and precise. The physical meaning behind the probability of instability is apparent, and overconservative or insufficiently robust designs can be avoided. Applications of stochastic robustness to analyzing full-state feedback aircraft control systems were described in [4]. The results presented there illustrated the use of stochastic stability robustness techniques in comparing control system designs and in including finite-dimensional uncertain dynamics.

Concepts behind stochastic stability robustness can be easily extended to provide insight into control system design for performance. Design specifications such as rise time, overshoot, settling time, dead time, and steady-state error are normally used as indicators of adequate performance and lend themselves to the same kind of analysis as described above. Concepts of stochastic stability robustness analysis can be

applied to these criteria giving probabilistic bounds on individual scalar performance criteria. Metrics resulting from stability and performance robustness can be related to controller parameters, thus providing a foundation for design tradeoffs and optimization. Details of these extensions and uses of stochastic robustness are described in the following and are illustrated by means of an example.

STOCHASTIC STABILITY ROBUSTNESS

Stochastic stability robustness of a linear, time-invariant (LTI) system was described in [3] and is summarized here. Consider a LTI system subject to constant-coefficient control:

$$\dot{x}(t) = F(p)x(t) + G(p)u(t) \qquad (1$$

$$y(t) = H(p)x(t) \qquad (2$$

$$u(t) = u_C(t) - CH(p)x(t) \qquad (3$$

$x(t)$, $u(t)$, $y(t)$, and p are state, control, output, and parameter vectors of dimension n, m, q, and r, respectively, accompanied by conformable dynamic, control, and output matrices that may be arbitrary functions of p. $u_C(t)$ is a command input vector, and, for simplicity, the $(m \times n)$ control gain matrix C is assumed to be known without error. The n eigenvalues, $\lambda_i = \sigma_i + j\omega_i$, $i = 1$ to n, of the matrix $[F(p) - G(p)CH(p)]$ determine closed-loop stability. The control gain matrix C is designed using some nominal or "mean" value of the dynamic model, denoted F, G, and H, that represents $F(p)$, $G(p)$, $H(p)$ evaluated at the nominal parameter vector. The actual system has an unknown description, denoted F_A, G_A, and H_A that depends on the actual (unknown) value of the parameter vector p. Environment, variations in the nominal state, system failures, parameter estimation errors, wear, and manufacturing differences all can contribute to mismatch between the actual system and that used to design the controller. The parameter vector p is assumed to have a known or estimated probability density function, denoted $pr(p)$, that expresses the statistics of parametric uncertainty due to the above factors.

System stability requires that no eigenvalues have positive real parts. While the relationship between parameters and eigenvalues is complicated, estimating the probability of instability ($\hat{\mathbb{P}}$) of a closed-loop system from repeated eigenvalue calculation is a straightforward task. Using *Monte Carlo evaluation*, the closed-loop eigenvalues are evaluated J times with each element of p_j, $j = 1$ to J, specified by a random-number generator whose individual outputs are shaped by $pr(p)$. The probability-of-instability estimate becomes increasingly precise as J becomes large. Then,

$$Pr(stability) = \lim_{J \to \infty} \frac{N(\sigma_{max} \le 0)}{J} \qquad (4$$

and

$$Pr(instability) = \mathbb{P} = 1 - Pr(stability) \qquad (5$$

---

[*] Graduate student
[**] Professor

181

$N(.)$ is the number of cases for which all elements of σ, the vector of the real parts of the closed-loop eigenvalues, are less than or equal to zero, that is, for which $\sigma_{max} \leq 0$, where σ_{max} is the maximum real eigenvalue component in σ. For less than an infinite number of evaluations, the resulting Monte Carlo evaluation is an estimate, denoted $\hat{P}$.

Because P is a *binomial* variable (i.e., the outcome of each Monte Carlo evaluation takes on one of two values: *stable* or *unstable*) confidence intervals are calculated using the binomial test, where lower (L) and upper (U) intervals satisfy [5]

$$Pr(X \leq x-1) = \sum_{j=0}^{x-1}(J,j)\, L^j(1-L)^{J-j} = 1 - \frac{\alpha}{2} \quad (6$$

$$Pr(X \leq x) = \sum_{j=0}^{X}(J,j)\, U^j(1-U)^{J-j} = \frac{\alpha}{2} \quad (7$$

X is the actual number of unstable cases after J evaluations ($X = J\hat{P}$) and (J, x) is the binomial coefficient, $\frac{J!}{x!(J-x)!}$. Explicit approximations of the binomial test [6, 7] avoid an iterative solution of Eq. 6 and 7 for (L,U) and are accurate to within 0.1%. Confidence intervals for the unknown, true probability of instability are presented in more detail in [3].

Stochastic Stability Robustness of Systems with Estimators

Stochastic stability robustness analysis is easily extended to systems incorporating dynamic state estimators. Using F_A, G_A, and H_A as the actual system matrices and F, G, and H as the design system, state and estimator equations are [8]

$$\dot{x}(t) = F_A(p)x(t) + G_A(p)u(t) + L_A(p)w(t) \quad (8$$

$$\dot{\hat{x}}(t) = F\hat{x}(t) + Gu(t) + K[z(t) - H\hat{x}(t)] \quad (9$$

$$u(t) = u_c(t) - C\hat{x}(t) \quad (10$$

where $\hat{x}(t)$ is the estimated state, L is the disturbance input matrix, and K is the estimator gain matrix. The measurement is taken through the actual output matrix and can include measurement noise:

$$z(t) = H_A(p)x(t) + n(t) \quad (11$$

Stability of the full dynamic compensator is determined by the combined system. Substituting for the control in Eq. 8 and 9, the eigenvalues of the closed-loop system matrix F_{cl} must be in the left-half plane for stability:

$$F_{cl} = \begin{bmatrix} F_A & -G_AC \\ KH_A & F - GC - KH \end{bmatrix} \quad (12$$

In terms of the state (x) and error dynamics (x - $\hat{x}$), the coupling effect of mismatch on the closed-loop system is directly apparent [8]

$$F_{cl} = \begin{bmatrix} F_A - G_AC & -G_AC \\ (F-F_A) - (G-G_A) - K(H-H_A) & F - (G-G_A)C - KH \end{bmatrix} \quad (13$$

The effect of parametric uncertainty on stability robustness is computed by Monte Carlo evaluation of the eigenvalues of Eq. 10, with F(p), G(p), and H(p) substituted for F_A, G_A, and H_A. Closed-loop eigenvalue densities portrayed on the

stochastic root locus show the possible interaction of dynamic and estimator states, and the possible robustness degradation due to the estimator. Well-known loss of LQ stability margins when a state estimator is added [9] can be quantified by the probability of instability.

STOCHASTIC PERFORMANCE ROBUSTNESS

While stability is an important element of robustness analysis, performance robustness analysis is vital to determining whether important design specifications are met. Stochastic stability robustness is described by a single parameter, the probability of instability. Adequate performance -- initial condition response, response to commanded inputs, control authority, and rejection of disturbances is difficult to describe by a single scalar. However, elements of stochastic stability robustness analysis (e.g., Monte Carlo evaluation and use of the tests described above for confidence intervals) apply independent of the performance criteria chosen. This will be demonstrated in the sequel.

Numerous criteria stemming from classical control concepts exist as measures of adequate performance. Appealing to these, one can begin a smooth transition from stability robustness analysis to performance robustness analysis simply by analyzing the *degree of stability* or *instability* rather than strict stability. As described in [3], one method of doing this is to shift the vertical discriminant line from zero to Σ less than (or greater than) zero (Fig. 1a). Histograms and cumulative distributions for varying degrees of stability are readily given by the Monte Carlo estimate of $1 - \int_{-\infty}^{\Sigma} pr(\sigma)d\sigma$,

where Σ represents a maximum real eigenvalue component, and $-\infty < \Sigma < \infty$. The histogram is a plot of $\frac{N[(\Sigma - \Delta) < \sigma_{max} \leq \Sigma]}{J}$ vs. Σ; Δ is an increment in Σ, $N[.]$ is the number of cases whose maximum real eigenvalue components lie in the increment, and J is the total number of evaluations. The histogram estimates the *stability probability density function*, $pr(\Sigma)$, which is obtained in the limit for a continuous distribution of Σ as $\Delta \to 0$ and $J \to \infty$. The *cumulative probability distribution of stability*, $Pr(\Sigma)$, is similarly estimated and presented as $\frac{N(\sigma_{max} \leq \Sigma)}{J}$ vs. Σ, the exact distribution being achieved in the limit as $J \to \infty$. Binomial confidence intervals are applicable to each point of the cumulative distribution, as there are just two values of interest, e.g., "satisfactory" or "unsatisfactory". The probability of instability is a special case where Σ equals zero.
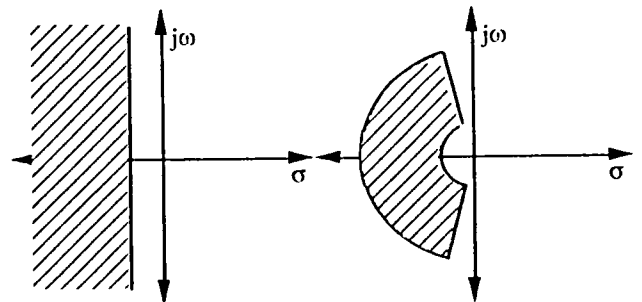

Figure 1 Alternate regions for probability of closed-loop eigenvalue location to aid in robustness analysis of transient response.
a) Alternate discriminant
b) Sector defined along lines of constant damping and natural frequency.

The measure of robustness resulting from the cumulative probability distribution is directly related to classical concepts

of rates of decay (growth) of the closed-loop response, time-to-half and time-to double:

$$t_{half} = \frac{0.693}{\zeta\omega_n} \tag{14}$$

$$t_{double} = -\frac{0.693}{\zeta\omega_n} \tag{15}$$

Taking degree-of-stability analysis one step further, rather than a vertical discriminant line, one can confine the closed-loop roots to *sectors in the complex plane* bounded by lines of constant damping and lines of constant natural frequency (Fig. 1b). Roots confined to these sectors would be expected to display a certain transient response speed. Again, the probability of roots lying within a sector is a binomial variable, and confidence interval calculations presented above apply.

While the speed of the transient response depends on the closed-loop poles, its magnitude and overall shape depends on the coefficients of the characteristic exponential and sinusoidal terms. Closed-loop zeros, residues, eigenvectors, and steady-state response are all concepts related to the magnitude of the response. The distribution of closed-loop zeros, of residues, of steady-state response, and of important elements of the eigenvectors all can be estimated by Monte Carlo analysis. Hence, a qualitative idea of the possible closed-loop responses can be obtained without calculating actual time responses.

Time responses provide the most clear-cut means of evaluating performance, but they are the most computation-intensive means as well. If actual time-responses are computed, stochastic performance robustness can be portrayed as a distribution of possible trajectories around a nominal or desired trajectory. After defining "envelopes" around the nominal trajectory (Fig. 2), the probability of violating the envelopes can be computed using Monte Carlo evaluation. The envelope chosen around the nominal trajectory encompasses scalar performance measures; the trajectories in Fig. 2 are examples of bounds defined by minimum and/or maximum allowable dead time, delay time, rise time, time to peak overshoot, peak overshoot, settling time, and steady-state error. While it is simple to conclude that a response violates such an envelope, individual responses within the envelope may not be acceptable. In such cases, the derivative of a response and envelopes around the derivative also can be used as performance criteria.
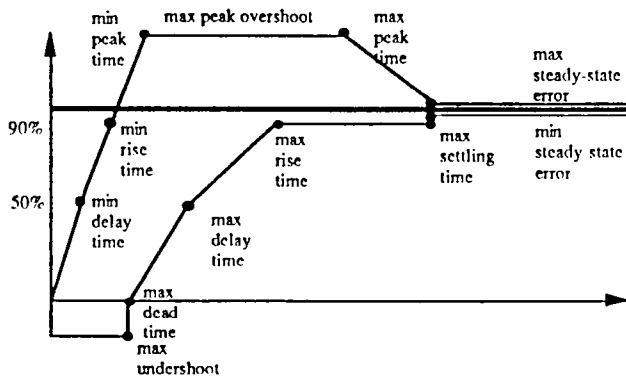

Figure 2. Example of step response bounds formed by scalar performance characteristics.

There is no unique set of criteria defining envelopes that bound an acceptable time response; the segmented envelopes in Fig. 2 can be smoothed, or other scalars can be used to define points on the envelope. However, once an envelope is defined, time response distributions can be computed by Monte Carlo methods. The closed-loop time response to a command

input, disturbance, initial condition, or some combination is evaluated J times, and for each evaluation, the trajectory is a binomial variable; it either stays within the envelope or violates the envelope. Although computing actual time responses is more computation-intensive than probability-of-instability estimation or estimation of scalar values associated with performance robustness, such analysis is well within the capability of existing workstations.

STOCHASTIC ROBUSTNESS AS A CONTROL DESIGN AID

Stochastic robustness metrics can and should be related to control system design parameters for robust control system design. While general "rules of thumb" regarding the design of robust control systems are useful, stochastic robustness metrics can identify non-obvious robustness "structures" of particular applications. Figure 3 illustrates tradeoffs that can exist and be uncovered by stochastic robustness analysis. Consider Fig. 3a, which shows the upper-half plane of a plant that has a complex pair of poles and a right-half-plane zero. Hypothetical "uncertainty circles" are drawn around possible closed-loop-root locations. As gain increases along the root locus, the uncertainty is magnified, and stability robustness decreases, with possible closed-loop root locations in the right-half plane at high enough gain. This case illustrates one where the decrease in robustness may be monotonic. Figure 3b postulates a system with a real pole and a complex pair of poles and zeros. In Fig. 3b, the hypothetical root locus nears the jω axis before ending at the zero in the left-half plane. Again, uncertainty circles enlarge as gain increases. In this case, it is possible that the root distributions cross into the right-half plane, yet are entirely in the left-half plane as gain increases further. Here, stability robustness (as measured by the probability of instability) may have local or global minima (as a function of gain). For multivariable systems with many parameters, the intrinsic structure of the problem and the tradeoff between the spread in closed-loop-root-location uncertainty versus the magnitude of the control gains may not be immediately evident. Plots of stochastic robustness metrics versus scalar control design parameters provide the necessary insight.
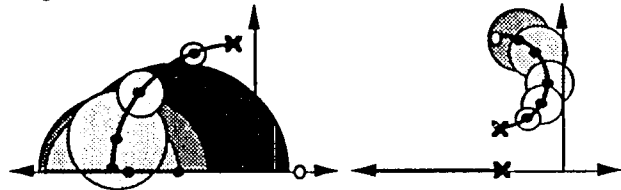

Figure 3 Illustration of design insight revealed by stochastic robustness analysis. Solid points indicate closed-loop eigenvalues enclosed by "uncertainty circles".
a) Root locus sketch where stability robustness decreases monotonically with increased gain.
b) Root locus sketch where stability robustness decreases then increases with increased gain.

EXAMPLE: SINGLE LINK ROBOT ARM

As an example of the concepts discussed above, stochastic robustness is applied to the flexible one-link robot described in Ref. 10. The model retains the first three flexible modes, and the tip of the link is controlled by applying a control torque to the hub, or base of the link. Because the structure of this model is representative of a general flexible structure, and the physical parameters are easily identifiable, it is a good candidate for stochastic robustness analysis.

The dynamic, control effect, and output matrices are given by

$$F = \begin{bmatrix} 0 & 1 & 0 & 0 & 0 & 0 & 0 & 0 \\ 0 & 0 & 0 & 0 & 0 & 0 & 0 & 0 \\ 0 & 0 & 0 & 1 & 0 & 0 & 0 & 0 \\ 0 & 0 & \omega_1^2 & -2\zeta_1\omega_1 & 0 & 0 & 0 & 0 \\ 0 & 0 & 0 & 0 & 0 & 1 & 0 & 0 \\ 0 & 0 & 0 & 0 & \omega_2^2 & -2\zeta_2\omega_2 & 0 & 0 \\ 0 & 0 & 0 & 0 & 0 & 0 & 0 & 1 \\ 0 & 0 & 0 & 0 & 0 & 0 & \omega_3^2 & -2\zeta_3\omega_3 \end{bmatrix} \tag{16}$$

$$G = \frac{1}{I_T}\begin{bmatrix} 0 \\ 1 \\ 0 \\ \phi_1'(0) \\ 0 \\ \phi_2'(0) \\ 0 \\ \phi_3'(0) \end{bmatrix} \quad H = \begin{bmatrix} L & 0 & \phi_1(L) & 0 & \phi_2(L) & 0 & \phi_3(L) & 0 \\ 0 & 1 & 0 & \phi_1'(0) & 0 & \phi_2'(0) & 0 & \phi_3'(0) \end{bmatrix} \tag{17,18}$$

where x is the length along the arm, $\phi_i(x)$, are the normal modes, $\phi_i' = \frac{d\phi_i}{dx}$, L is the length of the arm, and I_T is the total inertia of the arm. The measurements taken through H are the tip displacement and hub-rate, respectively. The flexibility of the open-loop system is apparent in the open-loop eigenvalues, which are $0, 0, -0.177 \pm 11.81j, -0.432 \pm 21.61j$, and $-0.968 \pm 48.37j$. The system has a readily identifiable 14-element parameter vector:

$$\mathbf{p} = [\zeta_1\ \omega_1\ \zeta_2\ \omega_2\ \zeta_3\ \omega_3\ \phi_1'(0)\ \phi_2'(0)\ \phi_3'(0)\ L\ \phi_1(L)\ \phi_2(L)\ \phi_3(L)\ I_T] \tag{19}$$

Details concerning the modeling and parameter identification are given in [10]. The linear-quadratic-regulator designed in [10] was used for demonstration and review of stochastic stability robustness analysis. The quadratic performance index weights tip position and tip-rate, and the LQR state-weighting and control-weighting matrices are

$$Q = 0.01 F^T H^T \begin{bmatrix} 1 & 0 \\ 0 & 0 \end{bmatrix} H F + H^T \begin{bmatrix} 1 & 0 \\ 0 & 0 \end{bmatrix} H, \quad R = 0.001 \tag{20, 21}$$

resulting in linear-quadratic regulator gains

$$C = [35.42\ 13.38\ 41.24\ 2.65\ 59.32\ -0.67\ 135.46\ 1.58] \tag{22}$$

and closed-loop eigenvalues $-5.41 \pm 48.8j, -6.47 \pm 23.8j, -6.1 \pm 2.66j, -7.7 \pm 11.42j$.

A uniform probability density function was chosen to model the parameter uncertainty statistics, with variations between $\pm 2\%$ of the nominal values for L and I_T and $\pm 25\%$ for the remaining parameters. The stochastic root locus for 50,000 evaluations of the full-state feedback case is given in Fig. 4. The nominal eigenvalues are marked, and the possible distribution is indicated by the height above the complex plane in units of roots/length along the real axis and roots/area in the complex plane. The "bin" size in Fig. 4 is 0.9 along the axis and 0.9 x 0.9 off of the axis. The probability of instability estimate ($\hat{P}$) for 50,000 evaluations is zero. Each of the four complex eigenvalue pairs appears in Fig. 4 as a "peak", with some distribution around the peak due to parametric uncertainty. The peaks can be well-defined (as in the lowest frequency complex pair) or broad (as in the highest frequency complex pair), and the nominal eigenvalues are not necessarily at the peaks of the distributions. Uncertainties of the magnitude chosen cause complex pairs to coalesce into real roots resulting in a distribution along the real axis.

Degree of stability is portrayed in Fig. 5 by the histogram and cumulative distribution of stability around the origin for a bin size of 0.25. (The smaller bin size was chosen for better resolution.) For binary parameter variations [3] of the same magnitude as the maximum uniform variations, 2^{14} or 16,384 deterministic evaluations give a zero probability of instability as well. These results indicate good stability robustness in the face of reasonably large uncertainties.

Moving to performance robustness analysis, Fig. 6 shows a top, contour-shaded view of a stochastic root-locus with sector bounds defined by $4 \leq \omega_n \leq 65$ and $\zeta > 0.1$. For 50,000 evaluations, the probability of having closed-loop eigenvalues outside of these bounds is 0.0147, with 95% confidence intervals (L,U) = (0.0136,0.0158). While the shape of the time response depends on closed-loop zeros, a minimum speed of response can be guaranteed by requiring that all closed-loop eigenvalues lie within a specified sector.

Figure 7a presents example step response envelopes and the response of the tip to a 4.8 cm position command input for 500 Monte Carlo evaluations. The control time history corresponding to the mean response is given in Fig. 7b. The transfer function between hub torque and tip position is non-minimum phase; thus the step response exhibits an initial response in the wrong direction. The time response envelopes in Fig. 7 indicate the maximum acceptable non-minimum phase response. For 500 responses, the probability of violating the time response envelope is 0.184 with 95% confidence intervals (L,U) = (0.151,0.221). Individual responses characteristic of those evaluated by Monte Carlo analysis are given in Fig. 8. While the responses fill out the envelope, some of the individual responses within the envelope may not be acceptable in the face of real-world criteria governing rate of change of the response (Fig. 8c). This is a case where checking envelopes around the derivative of the response may be necessary. Similar analyses can be performed on control trajectories to make sure bandwidth and control effort limitations are not violated during the simulation.

It is instructive from a design standpoint to plot stochastic robustness measures versus design parameters used to calculate feedback gains. Since there is only a single control in this example, the control weighting matrix R is a scalar and can be used as the design parameter. Two stochastic performance robustness measures are plotted versus R in Fig. 9 - the probability of violating the time response envelope and the probability of degree of instability. As control gains increase, the closed-loop roots are pushed farther into the left half plane, but they tend to migrate farther from their nominal values as well. At some value of control gain, there is a tradeoff between how far roots migrate and their location in the left half plane; thus a local minimum is apparent around R = 0.001 in the probability-of-degree-of-instability curves. While degree of instability improves for very small R, the control gains for this case are unrealistically large. For larger R (smaller control gains), the nominal closed-loop roots have real parts in the range of the values of Σ used; thus the probability of degree of instability increases rapidly beyond R = 0.01. The probability of the violating time response envelopes takes on the same shape as a function of R as the probability of degree of instability. In this example, the probability of instability is zero for all values of R checked, however, minima in the probability of instability versus design parameter curve can occur as well [11].

Figure 10 shows the stochastic root locus for the LQG system with estimator gains based on disturbance effect matrix $L = G$ and disturbance and noise covariance matrices

$$W = 1, \quad N = \begin{bmatrix} 0.005 & 0 \\ 0 & 10 \end{bmatrix} \tag{23, 24}$$

184

With estimator states added, the stochastic root locus changes in overall character from the full-state feedback case. Peaks are sharper, and the distribution along the real axis is less pronounced. In particular, note the eigenvalues associated with the largest peaks. In the full-state feedback system (Fig. 4) a broad distribution is associated with these eigenvalues, yet in Fig. 10, this pair of eigenvalues undergo very little variation from their nominal values! While the extent of the distribution into the left half plane is about the same as in Fig. 4, LQG system eigenvalues do migrate into the right half plane. The probability of instability estimate and 95% confidence intervals for 50,000 evaluations are $\hat{P}$ = 0.0771, and (L,U) = 0.0748, 0.0795, representing a significant loss in the stability robustness characteristic of the LQR system. These results reflect the well known fact that guaranteed stability margins of an LQR system are lost when an estimator is added.

Loop Transfer Recovery (LQG/LTR) [12] is a common design technique by which the trade-off between estimator performance and stability robustness can be made systematically using a single design parameter. Figure 11 illustrates the LTR mechanism for this example using the probability of instability as the robustness measure. Here plotting the probability of instability as a function of design parameter v ($W = vW_0$) shows that there is a value of v (v = 2) that minimizes the probability of instability. The fact that such a minimum exists may not be apparent by simply examining the estimator eigenvalues. The kind of results presented in Fig. 11 offer design insight and show robustness characteristics not revealed by other robustness metrics.

CONCLUSIONS

Stochastic robustness offers a rigorous yet straightforward alternative to current metrics for control system robustness that is simple to compute and is unfettered by normally difficult problem statements, such as non-Gaussian statistics, products of parameter variations, and structured uncertainty. Principles behind stochastic robustness can be applied to scalar performance metrics as well as time responses, making it a good candidate for overall robustness analysis. Both performance and stability metrics resulting from stochastic robustness analysis can provide details relating robustness characteristics intrinsic to a given application and scalar control design parameters, making it a good candidate for optimization techniques as well.
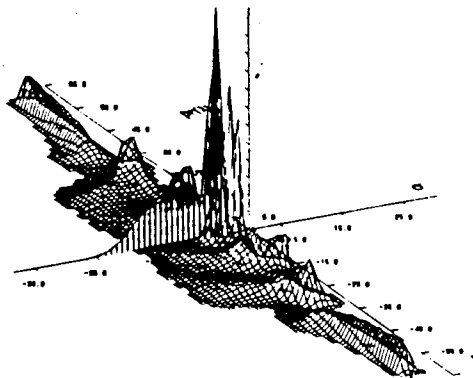
ACKNOWLEDGMENTS

REFERENCES

1) Stengel, R.F., "Some Effects of Parameter Variations on the Lateral-Directional Stability of Aircraft," AIAA Journal of Guidance and Control, Vol. 3, No. 2, pp. 124-131, Apr 1980.

2) Stengel, R.F., and Ryan, L.E., "Stochastic Robustness of Linear Control Systems", Proceedings of the 1989 Conference on Information Sciences and Systems, pp. 556-561, March, 1989.

3) Stengel, R.F., and Ryan, L.E., "Multivariate Histograms for Analysis of Linear Control System Robustness", American Control Conference Proceedings, pp. 937-943, Pittsburgh, PA, June 1989.

4) Ryan, L.E., and Stengel, R.F., "Application of Stochastic Robustness to Aircraft Control Systems", AIAA Guidance, Navigation and Control Conference Proceedings, pp. 698-708, Boston, Mass, Aug, 1989.

5) Conover, W.J., Practical Non-parametric Statistics, John Wiley and Sons, New York, 1980.

6) Anderson, T.W., and Burnstein, H., "Approximating the Upper Binomial Confidence Limit", Journal of the American Statistical Association, Vol. 62, pp. 857-861, Sept 1967.

7) Anderson, T.W., and Burnstein, H., "Approximating the Lower Binomial Confidence Limit", Journal of the American Statistical Association, Vol. 63, pp. 1413-1415, Dec 1968.

8) Stengel, R.F. Stochastic Optimal Control: Theory and Application, John Wiley and Sons, New York, 1986.

9) Doyle, J.C., "Guaranteed Margins for LQG Regulators," IEEE Transactions on Automatic Control, Vol. AC-23, No. 4, pp. 756-757, Aug 1978.

10) Cannon, R.J., and Schmitz, E., "Initial Experiments on the End-Point Control of a Flexible One-Link Robot", The International Journal of Robotics Research, Vol. 3, No. 3, pp. 62-75, Fall, 1984

11) Stengel, R.F., and Ryan, L.E., "Stochastic Robustness of Linear Time-Invariant Systems", to appear in IEEE Transactions on Automatic Control.

12) Doyle, J.C., and Stein, G., "Multivariable Feedback Design: Concepts for a Classical/Modern Synthesis," IEEE Transactions on Automatic Control, Vol. AC-26, No. 1, pp. 4-16, Feb 1981.

Figure 4 Stochastic root locus for the single-link robot with uniform parameters, 50,000 evaluations.
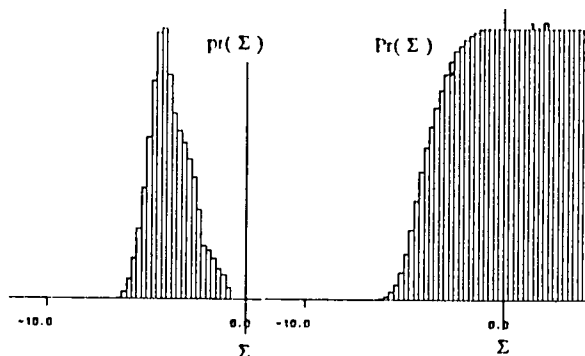

Figure 5 Histogram and cumulative distribution for the single-link robot with uniform parameters, 50,000 evaluations.
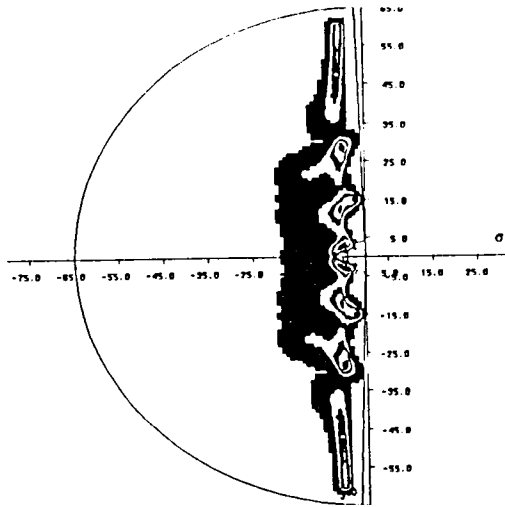
Figure 6 Top view of a stochastic root locus with sector bounds for the single-link robot, 50,000 evaluations.
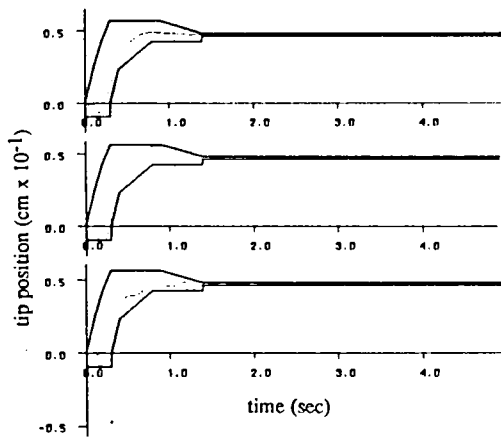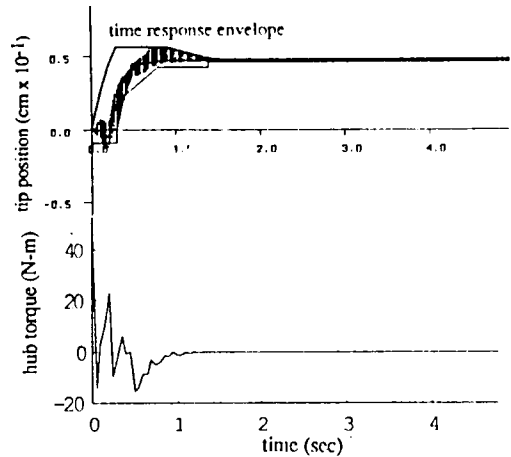

Figure 7 Time histories associated with tip position command of 4.8 cm.
a) 500 Monte Carlo evaluations of the tip response. Envelopes are defined by scalar performance criteria. Nominal response is indicated by the solid line.
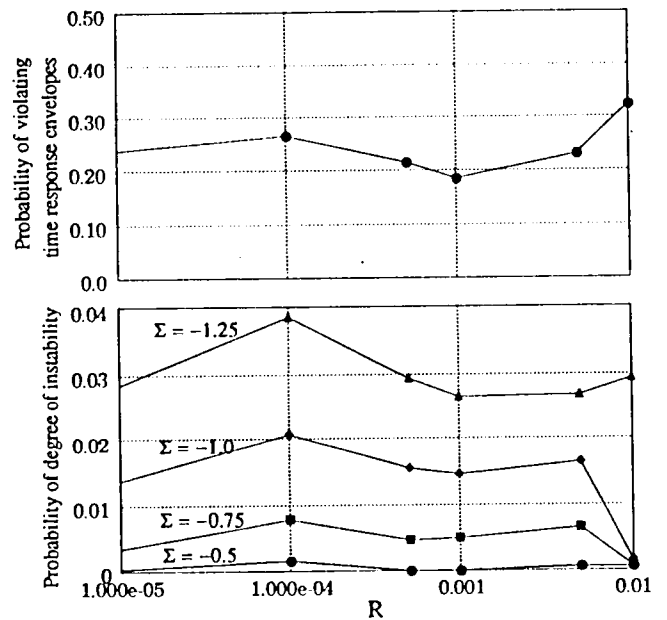b) Nominal control input.

Figure 8 Examples of individual tip responses
a) Acceptable response within envelope.
b) Response violates envelope.
c) Response is within envelope, but criteria governing its derivative may be required.
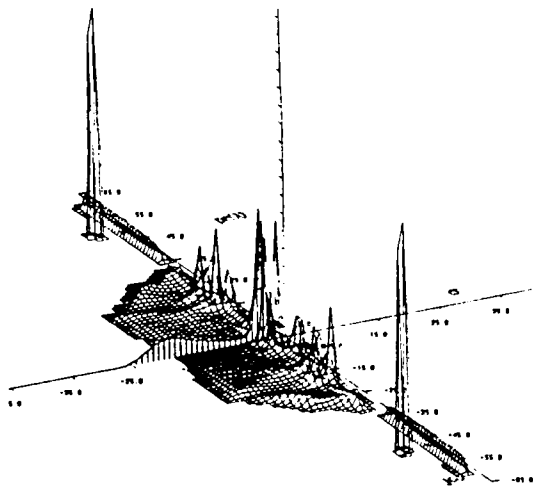
Figure 10 Stochastic root locus for the single-link robot with state estimation (LQG), 50,000 evaluations.

Figure 9 Stochastic performance robustness metrics vs. control weighting matrix R.
a) Probability of violating time response envelopes.
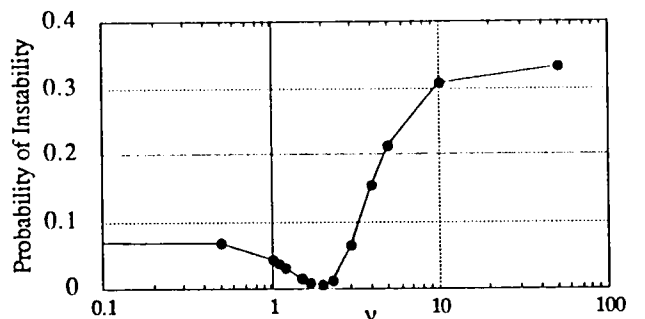b) Probability of degree of instability, for values Σ along the real axis.

Figure 11 Probability of Instability vs. LQG/LTR design parameter v.

186